Research Paper
J. Astron. Space Sci. 42(3), 63-76 (2025)
https://doi.org/10.5140/JASS.2025.42.3.63

JASS Journal of Astronomy and Space Sciences

Main Oscillatory Polar Motion of the Earth and Its Excitation: Investigation in Both the Frequency and Time Domains

Sung-Ho Na[1,2†], Yu Yi[3]

[1]Research Institute of Natural Sciences, Chungnam National University, Daejeon 34134, Korea
[2]Solbridge International School of Business, Woosong University, Daejeon 34613, Korea
[3]Department of Astronomy and Space Science, Chungnam National University, Daejeon 34134, Korea

Two main components of polar motion are Chandler wobble and annual wobble. Annual wobble is obviously caused by the seasonal perturbations on the Earth – such was suspected as well as readily confirmed in unison. Unlike annual wobble the cause of Chandler wobble has long been controversial, and finally solid proof came out with recent polar motion reconstruction using fluid spheres excitation data. In this study, certain characteristics of two main oscillatory components of polar motion are investigated once again. First, with two kinds of datasets; (i) the polar motion time series and (ii) the Earth's fluid sphere excitation time series, the cause of the main oscillatory polar motion including Chandler wobble is investigated. Formerly such investigations have been mostly done in the frequency domain only. We attempted to construct of polar motion time series from excitation through a new procedure using Fourier transform and its inverse. Secondly, the minor effect of earthquakes on Chandler wobble has been also assessed by the same method with a simple empirical model for post seismic relaxation. Then we compared the constructed polar motion with the observed polar motion. Contrary to several former claims, the role of geomagnetic jerk as another driving force of Chandler wobble is declined. Reliable estimates of the period and quality factor of Chandler wobble are attained.

Keywords: polar motion, Chandler wobble, annual wobble, excitation

1. INTRODUCTION

The rotation of the Earth has been quite an intimate phenomenon to humankind. Star positions on the celestial sphere were used in navigation for centuries. Aside from the slow precession in space, the Earth's spin axis apparently drifts on its surface as well, and this movement is called polar motion. Accurate terrestrial reference frame requires the exact position of the Earth's pole. The 'Reference Pole' was determined as the mean pole position at the year 1900. The pole position on the Earth's surface is continuously changing and the two main oscillatory components of polar motion are Chandler wobble and annual wobble. Due to scientific interests and technological needs, polar motion has been investigated for decades. Among excellent related literatures, we hereby cite two: a classical monograph by Munk and MacDonald (Munk & MacDonald 1960) and one book chapter by Gross (Gross 2009).

Ever since the beginning stages of Earth rotation study, the annual wobble has been believed to be driven by seasonal perturbation in the Earth's fluid spheres (Munk & MacDonald 1960), and this has been repeatedly confirmed with growing observational data (for example, Gross et al. 2003; Na et al. 2018). Chandler wobble is the free Eulerian nutation mode of the Earth, and the cause for its existence have been controversial for a long time. Numerous studies were undertaken to understand the characteristics and cause of Chandler wobble. One monograph was composed of extensive discussions from different perspectives (Plag et al. 2005). With growing evidences, the role of the outer fluid

Received 14 JUL 2025 **Revised** 22 AUG 2025 **Accepted** 27 AUG 2025
†**Corresponding Author**
Tel: +82-10-7703-8707, E-mail: sunghona@cnu.ac.kr
ORCID: https://orcid.org/0000-0003-2004-0715

https://janss.kr pISSN: 2093-5587 eISSN: 2093-1409

spheres to maintain Chandler wobble had been suspected for a long time, however, its concrete proof in the time domain has not been done until two recent articles (Xu et al. 2024; Yamaguchi & Furuya 2024), but in most studies, only the investigations on their spectra have been done.

Seismic excitation of Chandler wobble has been investigated repeatedly (for example, Smylie & Mansinha 1968; Chao & Gross 1987). Although its amount could be calculated early in the 90s, it was difficult to isolate its effect from polar motion. The path of polar motion does not show abrupt discontinuity even at the occurrences of largest earthquakes, but the resultant changes in the Earth's inertia tensor and corresponding excitation of Chandler wobble do follow. In this study we attempt to approximately calculate the amount of Chandler wobble due to largest earthquakes since 1980.

As a candidate energy source of Chandler wobble, geomagnetic jerk has been formerly referred (for example, Gibert & Le Mouël 2008). Most of those studies tried to verify the relation between the phase change of Chandler wobble and the geomagnetic jerks observed from geomagnetic field. In this study we attempt to identify whether such causal relation exists. Also, we take advantage of recent numerical modelling of geomagnetic jerks (Aubert & Finlay 2019) for checking the order of magnitude of such effect.

The main objective of this report is to confirm the cause of the Earth's oscillatory polar motion - particularly Chandler wobble once again. Aiming that objective, the reconstruction of polar motion from information of fluid sphere excitation and earthquake excitation is attempted via a new procedure using Fourier transform of those excitations. Accurate estimation of the period T and quality factor Q of Chandler wobble is also sought once again: first direct inspection of the spectrum and secondly careful checking for optimal combination of the two parameters in the frequency domain by comparing two kinds of excitation spectrum (geodetic and fluid spheres). We performed calculations in both the frequency and time domains by using the traditional approach and new ones including our simple and convenient formulation. Secular movement of the pole associated with slow changes in the Earth's principal moment of inertia due to the glacial isostatic adjustment (post glacial rebound) or other causes is beyond our scope in this study.

2. DATA, METHODS AND RESULTS

Two coordinates (x_p, y_p) specify the pole position with respect to the Reference Pole.

We acquired the polar motion time series data EOP C04 from the International Earth Rotation and Reference Systems Service (IERS) (Bizouard & Gambis 2009). The motion of the pole on the Earth is counterclockwise, and its center has been slowly migrating to the southeast or east. An angle of 0.1 arcsec in Fig. 1 corresponds to 3.1 meters on the Earth's surface. The two main oscillatory components of polar motion are Chandler wobble and annual wobble, and coexistence of these two resulted in beating of polar motion

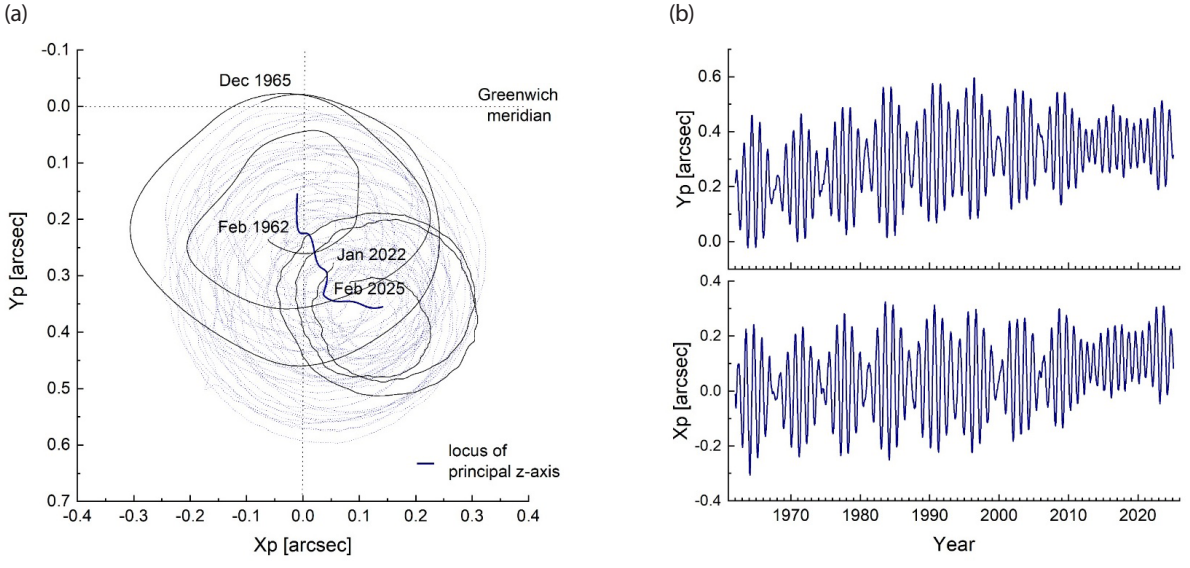

Fig. 1. Polar motion since 1962. (a) Pole position on the Earth's surface. The pole movement is clearly shown near the beginning and ending portions. The slowly changing principal axis of the Earth is shown over the whole polar motion locus. (b) Each time series of polar motion components x_p and y_p are shown. Data from IERS (2025).

time series of period about 6.4 yr. Although out of our scope, the secular drift of the Earth's pole has been another academic issue in geophysics and geodesy, and there also exist at least several minor periodicities in the polar motion.

2.1 Close Examination of Polar Motion Spectrum

The Fourier spectrum of the polar motion time series shown in Fig. 1, is illustrated in Fig. 2. On the Fig. 2(a), the amplitude spectrum $|P(\omega)|$ is drawn in logarithmic scale with distinction of the sense of rotation: prograde and retrograde. On the Fig. 2(b), the power spectrum $|P(\omega)|^2$ of the polar motion time series is illustrated for a period range of 330–480 days. Although the dominance of two components – Chandler and annual – is quite certain, there exist numerous minor components as shown in Fig. 2(a). It is noted that certain procedures; elimination of linear trend, proper tapering at both ends, and zero paddings were employed on the data time series before calculation of the Fourier spectrum through FFT.

The period range of Fig. 2(b) is narrowed for close inspection. The central periods of the two peaks are T = 1.185 yr (432.7 days) and T = 1 yr (almost exactly 365.24 days) for Chandler and annual wobbles. And the corresponding two half-widths are found as ΔT = 8.86 days and ΔT = 4.85 days respectively. For harmonic oscillator response under driving force of uniform amplitude, the quality factor is given as $Q = T / \Delta T$ (Fowles 1977). Under the same assumption we inferred two quality factors of Chandler and annual wobbles as Q = 49 and 75 respectively.

2.2 Polar Motion and Fluid Sphere Excitation

Since polar motion is free from external torques, the early formulation of polar motion and its excitation had been made by Munk & MacDonald (1960) starting from the law of angular momentum conservation. The current theory after developments continued was thoroughly documented by Gross (2009). A convenient relation between the polar motion and its excitation function can be written in the frequency domain as the following formula (Na et al. 2016).

$$(\Omega - \omega)P(\omega) = \Omega X(\omega) \tag{1}$$

where $P(\omega)$ and $X(\omega)$ are each Fourier transforms of complex polar motion $p_c = x_p - iy_p$ and complex excitation function $\chi_c = \chi_1 + i\chi_2$ respectively. In fact, this straightforward relation of Eq. (1) is the crucial connection between polar motion and excitation as will be shown below. The Chandler frequency is defined as $\Omega = \omega_0 (1 + 0.5i / Q) / T$, where ω_0 is the nominal value of the Earth's spin rotational angular velocity, and T and Q are the period and quality factor of Chandler wobble. Two components of polar motion excitation function are defined as follows.

$$\chi_i = \frac{1.608 h_i}{(C - A)\omega_0} + \frac{1.100 \Delta I_{i3}}{C - A} \quad (i = 1, 2) \tag{2}$$

where C and A are the two principal moments of inertia of the Earth, and h_i and ΔI_{i3} are the perturbing angular momentum and small changes in the Earth inertia tensor (Gross 2009). A brief derivation of Eqs. (1) and (2) is given in

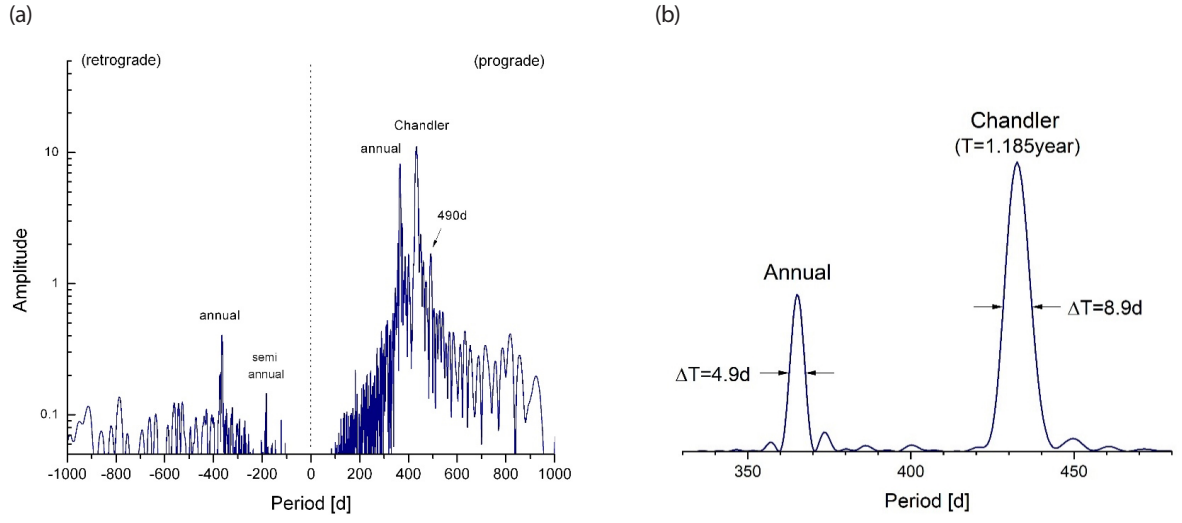

Fig. 2. Polar motion spectrum: (a) Amplitude spectrum in log scale with separation of prograde and retrograde components, (b) Power spectrum near the range of two dominant periodicities. Two half power widths are indicated by arrows.

Appendix 1. Explicit expressions for the excitation due to the atmospheric pressure and wind are shown in Appendix 2, which can be readily applied to evaluation of the excitation due to the ocean or the continental hydrosphere.

The perturbing roles of atmosphere and ocean on the Earth's rotation were studied with early data in the 1980s and 1990s. Among those foremost groups, are cited here as; Barnes et al. (1983), Salstein & Rosen (1989), Chao (1993), and Nastula & Ponte (1999). Since 2000, IERS has been publishing the three kinds of effective angular momentum due each to the atmosphere, ocean, and continental hydrosphere (Dobslaw et al. 2010). As a matter of fact, these datasets were provided by GFZ, and ESMGFZ datasets exist quite early from year 1976 and afterwards. In Fig. 3, two components χ_1 and χ_2 of the combined time series of three excitations together [atmo + ocean + hydro(con)] are shown. Two sets of each separate contributions from different fluid spheres are also shown in Appendix 2.

2.3 Geodetic Excitation Functions

The polar motion excitation can also be deduced from polar motion data by Eq. (1) via forward/inverse Fourier transformations. And this excitation function has been called 'geodetic excitation' to make a distinction from the excitation function estimated from the information on the Earth's fluid spheres. In fact, after comparison of two kinds of power spectra; fluid spheres excitation and geodetic excitation, Gross early addressed that 'there seems to be enough power to maintain Chandler wobble in the ocean and atmosphere together' (Plag et al. 2005). Yet such comparison has not been frequently made in the time domain except two cases (Xu et al. 2024; Yamaguchi & Furuya 2024). From comparison of the geodetic excitation (acquired for selected values of the two parameters T and Q of Chandler wobble) with fluid spheres excitation, one may determine optimal values of T and Q. Here the residual sum is defined as follows.

$$\Sigma\left|X_{aoh}(\omega)-X_{geod}(\omega)\right|^2 \tag{3}$$

where summation is carried for the frequency range of Chandler wobble. This sum of Eq. (3) has been repeatedly calculated in the ranges of 428 < T < 438 days and 0 < Q < 250. As a result, the optimal set: T = 433.2 days and Q = 62.8 has been found in this study and are illustrated in Fig. 4. In fact, we repeated calculations with different time windows for the optimal values. Our 1σ-interval estimates of period and quality factor are T = 433.2 ± 1.4 days and Q = 63 ± 17. Former estimates made by similar approach have varied as 429 < T < 432 days and 83 < Q < 107 (Gross 2009). It is noted here that we took care in the sum (3): (i) first separate the time series of daily basis into four ones of 4 day-interval (t=4k, 4k+1, 4k+2, 4k+3), (ii) perform Fourier transform for each separate time series, and (iii) add up the four each spectrum for each T and Q. In this way, the spectral resolution was enhanced four times. The Nyquist frequency is lowered accordingly, but that does not lead to any difficulty. This method was applied to both the fluid excitation and polar motion.

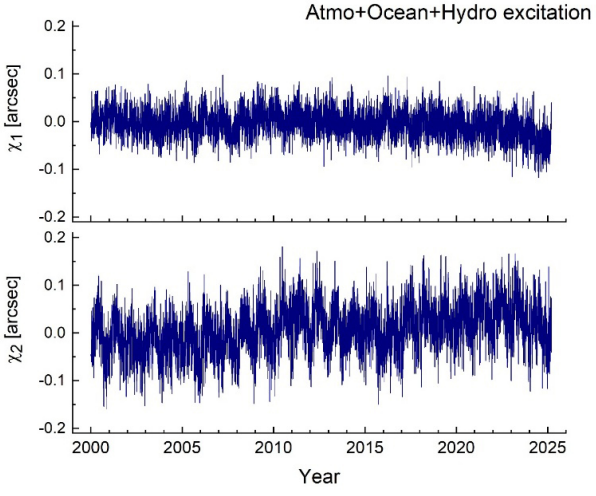

Fig. 3. Two components χ_1 and χ_2 of the combined polar motion excitation. These are the direct sum of the atmospheric, oceanic, and continental hydrosphere excitations. Data from IERS (2025).

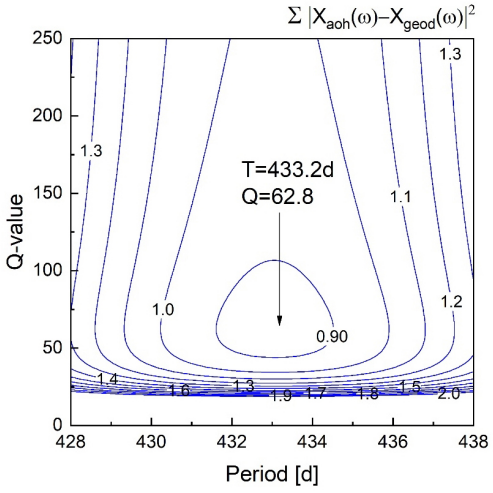

Fig. 4. Determination of Chandler wobble period and quality factor from minimum residual between fluid spheres excitation and geodetic excitation. Unit of the residual: [10^{-6} arcsec^2].

2.4 Excitation by Earthquakes: A Simple Empirical Model

For many decades earthquakes were regarded as possible energy sources of polar motion, particularly Chandler wobble. However, compared with damages at the Earth's surface or well-detected seismic waves, the perturbation of Earth's spin rotational state due to earthquakes is not quite noticeable. Dahlen derived the formula for the excitation in terms of seismic moment (Dahlen 1971, 1973). Lambeck compiled studies of Dahlen with other related ones, and noted the importance of aseismic excitation (Lambeck 1980). Gross and Chao calculated the seismic excitation on the polar motion (Gross 1986; Chao & Gross 1987; Gross & Chao 2006). Brzezinsky compiled and extended the formulation (Brzezinsky 2005). Smylie early addressed that large earthquakes should affect the pole position in discernable amount and later claimed that prediction of large earthquake can be made from the polar motion monitoring (Smylie & Mansinha 1968; Smylie & Zuberi 2009). However, seismic pole shifts are not large enough to be detected from polar motion observation, because the coseismic jump of the principal axis does not lead to discontinuity in the polar motion (Chung & Na 2016). Cambiotti et al. did extensive study to model polar motion due to earthquakes by using a new and elaborate scheme (Cambiotti et al. 2016). Xu and Chao renewed the estimate of seismic excitation and addressed that the cumulative seismic excitations should be accounted in the long-term polar motion (Xu & Chao 2019). By using an empirical relation, Na and Kyung approximately attained the effect of post seismic deformation unto the polar motion excitation by earthquakes (Hearn 2003; Na & Kyung 2016).

The procedure to calculate the coseismically excited polar motion for a single earthquake is followings: (i) first, evaluate seismic moment tensor M_{ij} for the earthquake, (ii) calculate the corresponding change in the Earth's rotational inertia tensor components ΔI_{13} and ΔI_{23}, (iii) calculate the excitation components (χ_1, χ_2) using Eq. (2), (iv) calculate the resultant coseismic polar motion using Eq. (1) (Fig. 5).

To evaluate polar motion excitation with assuming postseismic deformation is quite difficult task. One possible way is to adopt a homogeneous relaxation model and then apply it to assess polar motion excitation associated with it. Na & Kyung (2016) attempted this approach in their calculation of polar motion excitation due to earthquake including postseismic deformation. Their simple model for postseismic deformation was taken as follows,

$$u(t) = u_0 + u_1\left(1 - e^{-t/\tau}\right) \tag{4}$$

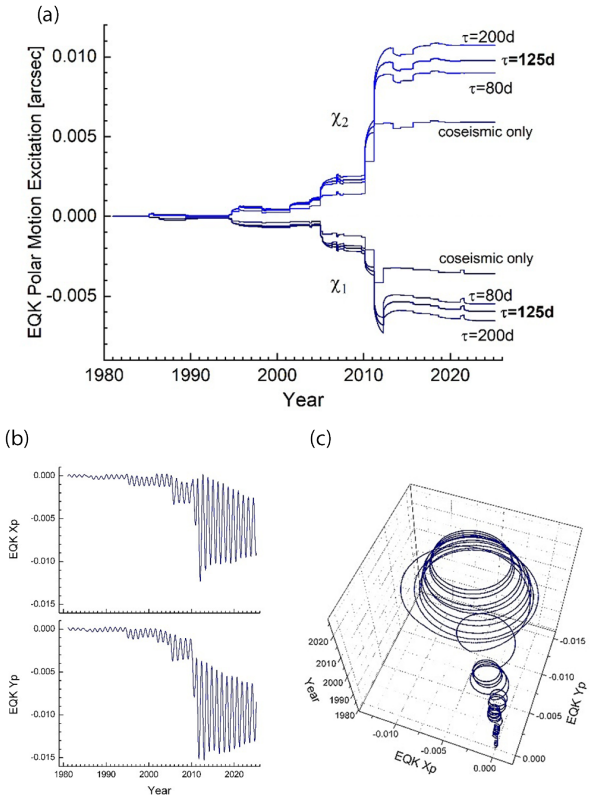

Fig. 5. Excited Chandler wobble due to largest earthquakes since 1980: (a) Two calculated components χ_1 and χ_2 of the polar motion excitation function by 37 largest earthquakes, (b) Two components of seismically excited Chandler wobble for assuming τ = 125 days, (c) 3-dimensional illustration of (b).

in which formula, the postseismic deformation is described as exponential decay with assigned characteristic time τ and the ratio between u_0 and u_1. The constants here were adopted as $u_1 = 0.655u_0$ for τ = 125 days. In fact, our choice of time constant here is the logarithmic mean value of two limits: τ = 80 days and τ = 200 days after Hearn (2003). The value $u_1 = 0.655u_0$ is determined by interpolation of two limiting values from fitting the observed crust relaxation after 2010 Tohoku Earthquake (Na & Kyung 2016). More theoretical details with parts of the calculated excitations are given in Appendix 3.

37 major earthquakes with magnitudes greater than 8 have occurred on the globe since 1981 until Feb 2025. Using the information of earthquakes from the USGS website, two components (χ_1, χ_2) of polar motion excitation function due to those earthquakes were assessed and are illustrated in Fig. 5(a). The illustrated three cases of excitations for assuming the post seismic deformation were calculated for the three characteristic relaxation time: 80, 125 and 200 days. The amounts of excitation increased by 52, 66 and 82 percents accordingly from the coseismic excitation. The greatest

coseismic excitation of polar motion was (–2.064, 2.356) milliarcsec for the 2011 Tohokou Earthquake in Japan. And the corresponding coseismic pole shift was 9.7 cm at the Earth's surface. The second largest coseismic pole shift was (–0.623, 0.561) milliarcsec for the 2004 Sumatra Earthquake. The seismically excited Chandler wobble due to those large earthquakes after 1980 is calculated and illustrated in Fig. 5(b) and 5(c). The polar motion excitation due to each earthquake is smaller than the combined excitation of atmospheric, oceanic, and hydrologic excitations by two orders of magnitude. The total effect of earthquakes with assuming post seismic relaxation is still smaller than the fluid spheres excitation by one order of magnitude.

2.5 Geomagnetic Jerk: Possibility of Another Excitation

It seems plausible that certain motion deep in the Earth's core should affect the rotation of the Earth. Geomagnetic jerk has been suspected as an energy source of Chandler wobble (Gibert & Le Mouël 2008; An & Ding 2022; and several references cited in them). We tried to confirm their findings that Chandler phase variation has been triggered by geomagnetic jerks. However, unlike their claims, the phase variation of Chandler wobble does not show close causal relationship with the jerks (Fig. 6).

According to Aubert & Finlay (2019), the amount of typical torque and time duration of geomagnetic jerk are approximately 1×10^{16} [Nm] and about 1 yr, which corresponds to angular momentum of 3.2×10^{23} [kg m^2 s^{-1}]. Since the spin rotational angular momentum of the Earth is 5.86×10^{33} [kg m^2 s^{-1}], two limiting cases can be assumed as follows: (i) torque exerts to deflect the Earth rotation axis, (ii) torque exerts to accelerate (decelerate) the earth rotation angular velocity. For the first case, the deflection angle will be 5.4×10^{-11} [rad], which corresponds to 0.34 mm at the surface of the Earth. With the second case $\Delta l.o.d = 4.6 \times 10^{-6}$ [sec]. Since these two simple calculations are for the maximum possible exertion of geomagnetic torque in each case, the truth would be smaller than these. Therefore, we do not agree with the former investigations addressing the possibility that Chandler wobble is significantly affected or driven by the geomagnetic jerks. The related details are given in Appendix 4.

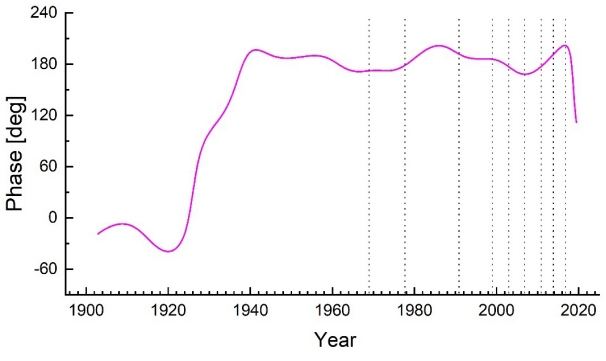

Fig. 6. Phase variation of Chandler wobble shown together with dotted lines at epochs of the known geomagnetic jerks.

2.6 Constructed Polar Motion: Comparison

From the known values of years-long polar motion excitation, one can deduce the corresponding polar motion by using the simple relation of the two Fourier transform pair in the frequency domain; Eq. (1). We then separately calculated the transient polar motion and added it unto the acquired polar motion after Eq. (1). Fig. 7 is a composite of two panels: (a) the constructed polar motion from the combination of atmospheric, ocean, and hydrologic excitations, (b) observed polar motion. The seismically excited polar motion is mostly of Chandler wobble period. For comparison with Fig. 7(a), the earthquake excited portion and secular movement have been deducted from the polar motion of Fig. 7(b). It is noted here that we initially acquired the fluid excitation time series data from IERS and calculated for only after year 2000. We learned the existence of original and longer dataset in ESMGFZ starting from 1976. The polar motion before 1981 is again omitted (constructed polar motion of these several year time span is much smaller and our seismic effect calculation starts in 1981).

The cause of polar motion as known as the combination of atmospheric, oceanic, and hydrologic effects is explicitly shown in Fig. 7; where the constructed polar motion is compared with the observed polar motion. Not only their amplitudes but also the waveforms of the two sets of time series (Fig. 7(a) and 7(b)) are comparable and in fair match to each other. However, the root mean square value of the difference between the constructed time series and the observed one is found 0.062 arcsec. Therefore, there still remains substantial misfit, which should be ascribed to the limited accuracy in the dataset of the fluid spheres states.

As noted above, atmospheric perturbation was early claimed as the cause of polar motion, and later oceanic and hydrologic effects were recognized. Dozens of studies then followed. However, for more than three decades, almost all those analyses were carried in the frequency domain only. Quite recently, there were two reports in which construction of polar motion is attempted (Xu et al. 2024; Yamaguchi & Furuya 2024). This was due to the shortage of dataset of fluid spheres excitation before 2000s, and also the difficulty

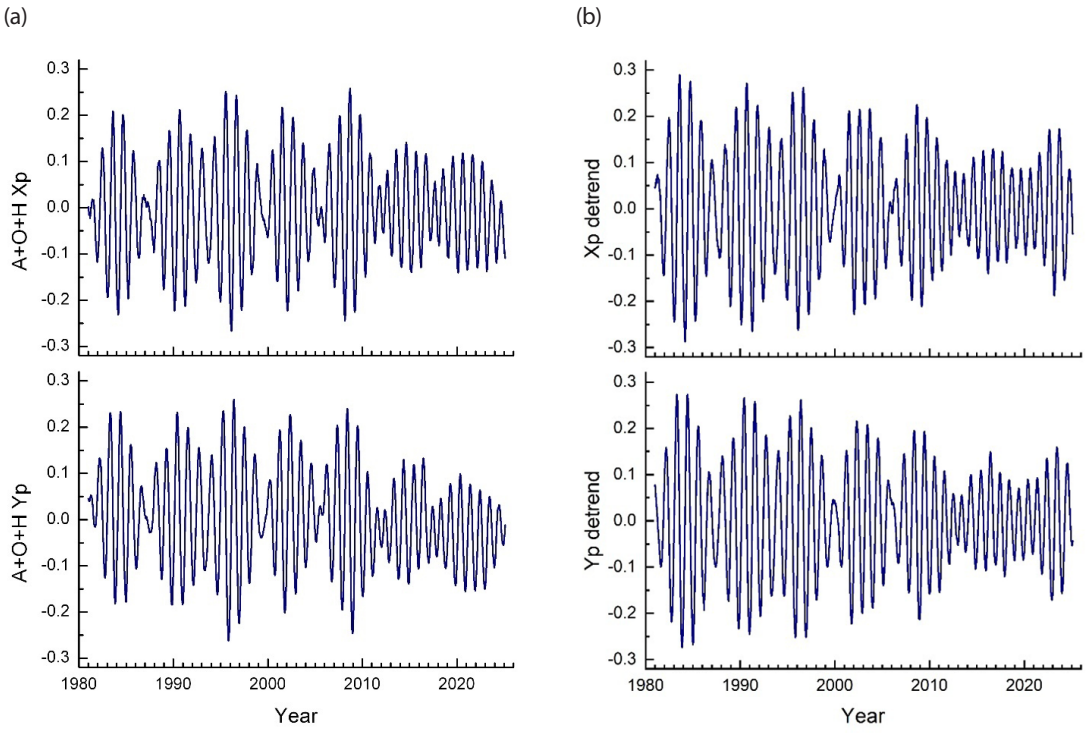

Fig. 7. Comparison of constructed and observed polar motion time series sets: (a) polar motion due to fluid spheres excitation (atmo + ocean + hydro), (b) observed polar motion devoid of follows; (i) slow trend of Earth's principal axis movement and (ii) earthquake excitation. Units of polar motion: [arcsec].

in integral evaluation of polar motion in the time domain (Barnes et al. 1983; Chao 1985).

We constructed polar motion for four more cases of different combination of parameters: period T and Q-value of Chandler wobble: (T, Q) = (437, 120), (429, 120), (429, 25), and (437, 25). The four pairs of these additionally constructed polar motions are illustrated in Fig. 8. We found that the corresponding misfit is increased in the r.m.s. value as 0.135, 0.087, 0.097 and 0.110 arcsec respectively.

3. DISCUSSION AND CONCLUSION

The followings are our concluding remarks: After assessments in both the frequency and time domain together, the Earth's outer fluid spheres excitation is clearly identified as the dominant cause of the oscillatory polar motion including Chandler wobble. Chandler period was found as 432.7 days from the Fourier spectrum of the recent polar motion. By modelling of geodetic excitation in the frequency domain, the period and quality factor of Chandler wobble has been estimated as T = 433.2 days and $Q \approx 63$. The minor contribution on Chandler wobble from earthquakes could be calculated, although seismic pole shifts themselves cannot be easily isolated on the polar motion. Effect of geomagnetic jerks on the Earth's polar motion is negligible.

Constructing polar motion from fluid spheres excitation will be improved in future with accumulation of accurate datasets. The fluid spheres excitation dataset might have underestimated its true values at times by about 10% or so. Still the two time series illustrated as Fig. 7(a) and 7(b) are comparable, and we hope the defect would be smaller with more accurate dataset in future. The difference between the observed polar motion and the constructed polar motion was minimum when the parameter set of (T = 433.2 days and Q = 62.8) was taken, compared with four other choices (Fig. 8). There is slow decrease in the constructed A + O + H yp time series in 7(a), which corresponds to gradual increase in hydrologic excitation after 2005 as shown in Fig. A1(b). Elaborate explanation about this slow excitation is included in one recent article (Seo et al. 2025). Actual Chandler wobble excited by the two greatest earthquakes were approximately calculated in this study as 37 cm and 9.5 cm in the wobble diameter (Fig. 5(b) and (c)).

The Chandler period itself should be regarded as an intrinsic property of the whole Earth structure, even though its observed value may slightly vary depending on the data time span and the method of investigation. Q-value estimate on the power spectrum in 2.1 is not rigorously valid for the polar motion, which is not a harmonic oscillation under

uniform driving force (see the spectra shown in Appendix 2). Post-seismic relaxation should not be neglected in seismic polar motion excitation, because the amount of Chandler component associated is large as about 60 percent of coseimic polar motion. There were reports of phenomena, rather than Chandler wobble, to have possible relation with geomagnetic jerks: (i) free core nutation phase change (Malkin et al. 2022), and (ii) Earth's spin angular velocity change of several year periodicities (Ding et al. 2021). Such two might not be artefacts but real signals associated with slow movement in the Earth's core.

ACKNOWLEDGEMENTS

This report has been financially supported by the Korea National Research Foundation (RS-2022-NR069941). The authors appreciate the datasets from IERS, GFZ, USGS and JPL, and also deeply appreciate valuable advices and suggestions from two reviewers. First author would like to dedicate this work in honor of Dr. Goad, C. (adviser deceased).

ORCIDs

Sung-Ho Na	https://orcid.org/0000-0003-2004-0715
Yu Yi	https://orcid.org/0000-0001-9348-454X

REFERENCES

An Y, Ding H, Revisiting the period and quality factor of the Chandler wobble and its possible geomagnetic jerk excitation, Geod. Geodyn. 13, 427-434 (2022). https://doi.org/10.1016/j.geog.2022.02.002

Aubert J, Finlay CC, Geomagnetic jerks and rapid hydromagnetic waves focusing at Earth's core surface, Nat. Geosci. 12, 393-398 (2019). https://doi.org/10.1038/s41561-019-0355-1

Barnes RTH, Hide R, White AA, Wilson CA, Atmospheric angular momentum fluctuations, length-of-day changes and polar motion, Proc. R. Soc. A Math. Phys. Eng. Sci. 387, 31-73 (1983). https://doi.org/10.1098/rspa.1983.0050

Bizouard C, Gambis D, The combined solution C04 for Earth orientation parameters consistent with international terrestrial reference frame 2005, in Geodetic Reference Frames: IAG Symposium, ed. Drews H (Springer, Berlin, 2009), 265-270.

Brzezinsky A, Review of Chandler wobble and its excitation, in Forcing of Polar Motion in the Chandler Frequency Band, eds. Plag HP, Chao B, Gross R, van Dam T (European Center of Geodynamics and Seismology, Luxemburg, 2005), 109-120.

Cambiotti G, Wang X, Sabadini R, Yuen DA, Residual polar motion caused by coseismic and interseismic deformations from 1900 to present, Geophys. J. Int. 205, 1165-1179 (2016). https://doi.org/10.1093/gji/ggw077

Chao BF, Excitation of Earth's polar motion by atmospheric angular momentum variations, 1980–1990, Geophys. Res. Lett. 20, 253-256 (1993). https://doi.org/10.1029/93GL00130

Chao BF, On the excitation of the Earth' polar motion, Geophys. Res. Lett. 12, 526-529 (1985). https://doi.org/10.1029/GL012i008p00526

Chao BF, Gross RS, Changes in the Earth's rotation and low-degree gravitational field induced by earthquakes, Geophys. J. Int. R. Astron. Soc. 91, 569-596 (1987). https://doi.org/

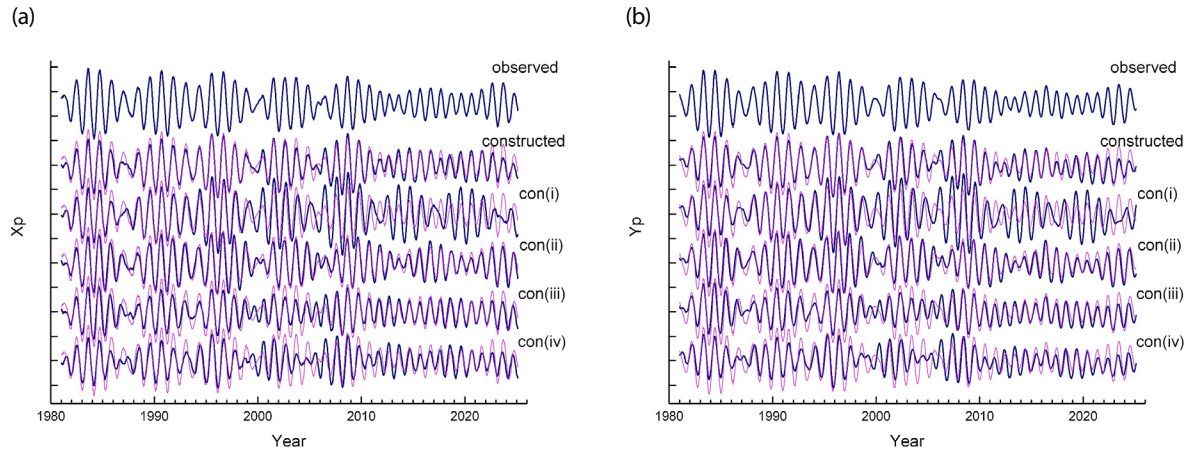

Fig. 8. More comparison between the observed polar motion and the constructed polar motion. Two components x_p and y_p are separately shown (a), (b). In both (a) and (b), from the top, observed polar motion and five constructed ones. 'con (i, ii, iii, iv)' stand for constructed with (T, Q) = (437, 120), (429, 120), (429, 25), and (437, 25). Duplicate observed polar motion in magenta (Unit: 0.2 arcsec).

10.1111/j.1365-246X.1987.tb01659.X

Chung TW, Na SH, A least square fit analysis on the Earth's polar motion time series: implication against Smylie's conjecture, Geophys. Geophys. Expl. 19, 91-96 (2016). https://doi.org/10.7582/GGE.2016.19.2.091

Dahlen FA, A correction to the excitation of the Chandler wobble by earthquakes, Geophys. J. Int. R. Astron. Soc. 32, 203-217 (1973). https://doi.org/10.1111/j.1365-246X.1973.tb06527.X

Dahlen FA, The excitation of the Chandler wobble by earthquakes, Geophys. J. Int. R. Astron. Soc. 25, 157-206 (1971). https://doi.org/10.1111/j.1365-246X.1971.tb02336.X

Ding H, An Y, Shen W, New evidence for the fluctuation characteristics of intradecadal periodic signals in length-of-day variation, J. Geophys. Res. Solid Earth. 126, e2020JB020990 (2021). https://doi.org/10.1029/2020JB020990

Dobslaw H, Dill R, Grötzsch A, Brzeziński A, Thomas M, Seasonal polar motion excitation from numerical models of atmosphere, ocean, and continental hydrosphere, J. Geophys. Res. Solid Earth. 115, e2009JB007127 (2010). https://doi.org/10.1029/2009JB007127

Fowles GR, Analytical Mechanics, 3d ed. (Holt, Rinehart and Winston, New York, 1977).

Gibert D, Le Mouël JL, Inversion of polar motion data: Chandler wobble, phase jumps, and geomagnetic jerks, J. Geophys. Res. Solid Earth. 113, e2008JB005700 (2008). https://doi.org/10.1029/2008JB005700

Gross RS, 3.09 - Earth Rotation Variations: Long Period, vol. 3, in Treatise of Geophysics, ed. Schubert G (Elsevier, Amsterdam, 2009), 239-294.

Gross RS, The influence of earthquakes on the Chandler wobble during 1977–1983, Geophys. J. Int. R. Astron. Soc. 85, 161-177 (1986). https://doi.org/10.1111/j.1365-246X.1986.tb05176.X

Gross RS, Chao BF, The rotational and gravitational signature of the December 26, 2004 Sumatran earthquake, Sur. Geophys. 27, 615-632 (2006). https://doi.org/10.1007/s10712-006-9008-1

Gross RS, Fukumori I, Menemenlis D, Atmospheric and oceanic excitation of the Earth's wobbles during 1980–2000, J. Geophys. Res. Solid Earth. 108, e2002JB002143 (2003). https://doi.org/10.1029/2002JB002143

Hearn EH, What can GPS data tell us about the dynamics of post-seismic deformation? Geophys. J. Int. R. Astron. Soc. 155, 753-777 (2003). https://doi.org/10.1111/j.1365-246X.2003.02030.X

International Earth Rotation and Reference Systems Service (IERS) (2025) [Internet], viewed 2025 Feb 20, available from: https://www.iers.org/IERS/EN/Home/home_node.html

Lambeck K, The Earth's Variable Rotation (Cambridge University Press, Cambridge, 1980).

Malkin Z, Belda S, Modiri S, Detection of a new large free core nutation phase jump, Sensors. 22, 5960 (2022). https://doi.org/10.3390/s22165960

Munk WH, MacDonald GJF, The Rotation of the Earth: A Geophysical Discussion (Cambridge University Press, London, 1960).

Na SH, Cho J, Kim TH, Seo K, Youm K, et al., Changes in the Earth's spin rotation due to the atmospheric effects and reduction in glaciers, J. Astron. Space Sci. 33, 295-304 (2016). https://doi.org/10.5140/JASS.2016.33.4.295

Na SH, Cho J, Seo KW, Youm KH, Shen W, A note on the annual wobble excitation due to the seasonal atmospheric loading on continents, Terr. Atmos. Ocean. Sci. 29, 721-729 (2018). https://doi.org/10.3319/TAO.2018.08.24.01

Na SH, Kyung JB, Perturbation in the Earth's pole due to the recent 31 large earthquakes of magnitude over 8.0, J. Korean. Ear. Sci. Soc. 37, 271-276 (2016). https://doi.org/10.5467/JKESS.2016.37.5.271

Nastula J, Ponte RM, Further evidence for oceanic excitation of polar motion, Geophys. J. Int. 139, 123-130 (1999). https://doi.org/10.1046/j.1365-246X.1999.00930.X

Plag HP, Chao BF, Gross RS, van Dam T, Forcing of polar motion in the Chandler frequency band: an opportunity to evaluate interannual climate variations (European Center of Geodynamics and Seismology, Luxemburg, 2005).

Salstein DA, Rosen RD, Regional contributions to the atmospheric excitation of rapid polar motions, J. Geophys. Res. Atmos. 94, 9971-9978 (1989). https://doi.org/10.1029/JD094iD07p09971

Seo KW, Ryu D, Jeon T, Youm K, Kim JS, et al., Abrupt sea level rise and Earth's gradual pole shift reveal permanent hydrological regime changes in the 21st century, Science. 387, 1408-1413 (2025). https://doi.org/10.1126/science.adq6529

Smylie DE, Mansinha L, Earthquakes and the observed motion of the rotation pole, J. Geophys. Res. 73, 7661-7673 (1968). https://doi.org/10.1029/JB073i024p07661

Smylie DE, Zuberi M, Free and forced polar motion and modern observations of the Chandler wobble, J. Geodyn. 48, 226-229 (2009). https://doi.org/10.1016/j.jog.2009.09.028

Xu CY, Chao BF, Seismic effects on the secular drift of the Earth's rotational pole, J. Geophys. Res. Solid Earth. 124, 6092-6100 (2019). https://doi.org/10.1029/2018JB017164

Xu XQ, Fang M, Zhou YH, Liao XH, Continental and oceanic AAM contributions to Chandler Wobble with the amplitude attenuation from 2012 to 2022, J. Geod. 98, 59 (2024). https://doi.org/10.1007/s00190-024-01872-z

Yamaguchi R, Furuya M, Can we explain the post-2015 absence of the Chandler wobble? Earth Planets Space. 76, 1 (2024). https://doi.org/10.1186/s40623-023-01944-Y

APPENDIX 1

Polar Motion and its Excitation: Brief Formulation

Write the angular velocity of the Earth as follows.

$$\vec{\omega} = \omega_0 \begin{bmatrix} m_1 \\ m_2 \\ 1+m_3 \end{bmatrix} \tag{A1}$$

where, m_i refers to small perturbation. Also write the perturbed inertia tensor of the Earth and the imposed perturbing angular momentum as follows.

$$\begin{bmatrix} A+\Delta I_{11} & \Delta I_{12} & \Delta I_{13} \\ \Delta I_{21} & A+\Delta I_{22} & \Delta I_{23} \\ \Delta I_{31} & \Delta I_{32} & C+\Delta I_{33} \end{bmatrix} \text{ and } \begin{bmatrix} h_1 \\ h_2 \\ h_3 \end{bmatrix} \tag{A2}$$

where C and A are the Earth's principal moments of inertia, and ΔI_{ij} and h_i are each component of the small perturbation in the inertia tensor and angular momentum. The relative amounts of perturbations are usually in the order of 10^{-7} or smaller, and therefore first order approximation is valid. Then the angular momentum can be written as follows.

$$\begin{bmatrix} L_1 \\ L_2 \\ L_3 \end{bmatrix} = \omega_0 \begin{bmatrix} Am_1 + \Delta I_{13} \\ Am_2 + \Delta I_{23} \\ C(1+m_3) + \Delta I_{33} \end{bmatrix} + \begin{bmatrix} h_1 \\ h_2 \\ h_3 \end{bmatrix} \tag{A3}$$

The angular momentum conservation for the rotating Earth is given as $\partial \vec{L}/\partial t + \vec{\omega} \times \vec{L} = 0$, from which the following coupled equations are derived.

$$\begin{aligned} \frac{1}{\Omega}\frac{dm_1}{dt} + m_2 &= \chi_2 - \frac{1}{\omega_0}\frac{d\chi_1}{dt} \\ \frac{1}{\Omega}\frac{dm_2}{dt} - m_1 &= -\chi_1 - \frac{1}{\omega_0}\frac{d\chi_2}{dt} \end{aligned} \tag{A4}$$

Two components of polar motion excitation function for the rigid Earth can be written as

$$\chi_i = \frac{h_i}{(C-A)\omega_0} + \frac{\Delta I_{i3}}{C-A} \quad (i=1,2) \tag{A5}$$

with the Euler free nutation frequency of the rigid Earth

$$\Omega = \frac{C-A}{C}\omega_0 \cong \frac{\omega_0}{305.46}. \tag{A6}$$

However, the most proper expression for the real Earth is given as follows.

$$\chi_i = \frac{1.608\, h_i}{(C-A)\omega_0} + \frac{1.100\,\Delta I_{i3}}{C-A} \quad (i=1,2) \tag{A7}$$

Also, the Chandler frequency is lowered by about 30 (29.5) percent due mainly to the elastic mantle and oceans. The axial component of excitation function for the rigid Earth is written as

$$\chi_3 = -m_3 = \frac{h_3}{C\,\omega_0} + \frac{\Delta I_{33}}{C}, \tag{A8}$$

which is modified for the real Earth as

$$\chi_3 = \frac{0.997 h_3}{C\,\omega_0} + \frac{0.748\Delta I_{33}}{C}. \tag{A9}$$

Define three complex functions $m_c = m_1 + im_2$, $p_c = x_p - iy_p$ and $\chi_c = \chi_1 + i\chi_2$. The angular velocity perturbation and polar motion are closely related as

$$m_c = p_c - \frac{i}{\omega_0}\frac{\partial p_c}{\partial t}. \tag{A10}$$

The complex Chandler frequency can be written as

$$\Omega = \frac{\omega_0}{T}\left(1 + \frac{i}{2Q}\right). \tag{A11}$$

Write $M(\omega)$, $P(\omega)$ and $X(\omega)$ as three each Fourier transforms of complex functions m_c, p_c and χ_c respectively, then we have a relation between them as follows.

$$(\Omega - \omega)P(\omega) = \frac{\omega_0}{\omega_0 + \omega}(\Omega - \omega)M(\omega) = \Omega\, X(\omega) \tag{A12}$$

Three references for Appendix 1 are Munk & MacDonald (1960), Gross (2009), and Na et al. (2016).

APPENDIX 2

Excitation by Outer Fluid Sphere

The perturbation ΔI_{i3} and h_i due to excessive mass and movement in the fluid outer spheres of the Earth can be acquired according to the formulae below. Although the formula for the perturbation ΔI_{i3} and h_i due to the atmosphere are shown here, similar perturbation due to the ocean and hydrosphere can be evaluated same way.

Perturbation in the off-diagonal inertia tensor components of the Earth associated with the atmospheric pressure distribution can be evaluated as follows.

$$\Delta I_{13} = -\frac{a^4}{g}\iint \Delta p(a)\ cos\theta\ sin^2\theta\ cos\varphi\ d\theta d\varphi$$
$$\Delta I_{23} = -\frac{a^4}{g}\iint \Delta p(a)\ cos\theta\ sin^2\theta\ sin\varphi\ d\theta d\varphi \quad \text{(A13)}$$

where $\Delta p(a)/g$ represents the local excessive air mass density on the Earth's surface.

The angular momentum associated with the global wind distribution can be evaluated as follows.

$$h_1 = \frac{a^3}{g}\iiint \Delta p(z)(-u\ sin\theta\ cos\theta\ cos\varphi + v\ sin\varphi)sin\theta\ dz\ d\theta\ d\varphi$$
$$h_2 = \frac{a^3}{g}\iiint \Delta p(z)(-u\ sin\theta\ cos\theta\ sin\varphi - v\ cos\varphi)sin\theta\ dz\ d\theta\ d\varphi \quad \text{(A14)}$$

where (u, v) are the eastward and northward wind velocity and $\Delta p(z)/g$ corresponds to the local excessive air mass density at height z. After evaluation of the perturbation ΔI_{i3} and h_i, the polar motion excitation is readily found by Eq. (2).

International Earth Rotation and Reference Systems Service (IERS) shows each time series of the polar motion excitation due to atmosphere, ocean, and hydrosphere since 2000, while the original ESMGFZ datasets are available from 1976. These datasets downloaded from the IERS website are illustrated in Fig. A1(a) and A1(b).

Two kinds of spectra: fluid spheres excitation spectrum and geodetic excitation spectrum have been acquired. From the fluid spheres excitation dataset shown in Fig. 3, we acquired its Fourier transform $X_{aoh}(\omega)$, of which power $|X_{aoh}(\omega)|^2$ is shown in Fig. A2(a). The geodetic excitation in

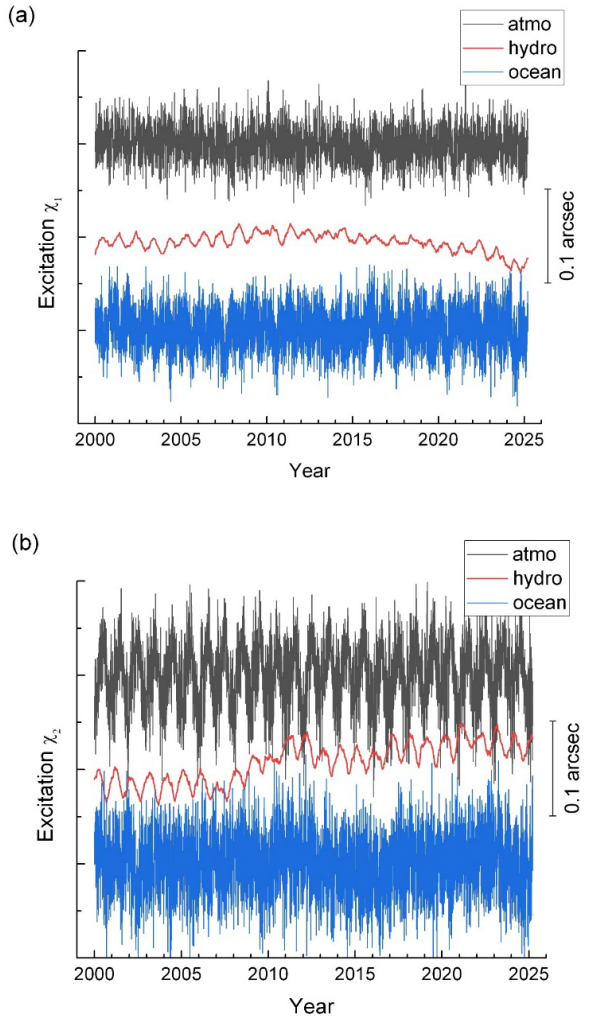

Fig. A1. Polar motion excitation due to atmosphere, ocean, and hydrosphere since 2000. Each contribution is separately shown in (a) and (b) for the two components (χ_1, χ_2). Data from IERS (2025).

frequency domain $X_{geod}(\omega)$ was calculated via Eq. (1) on the Fourier transform of polar motion shown in Fig. 1. Its power $|X_{geod}(\omega)|^2$ is shown in Fig. A2(b).

As illustrated in Fig. A2, the power of fluid spheres excitation is comparable to that of geodetic excitation in the long period range including the annual and Chandler wobble frequencies. However, in the higher frequency range (monthly to weekly), the geodetic excitation power is larger than the fluid spheres excitation. This difference should be caused by the limited accuracy of the fluid spheres excitation dataset.

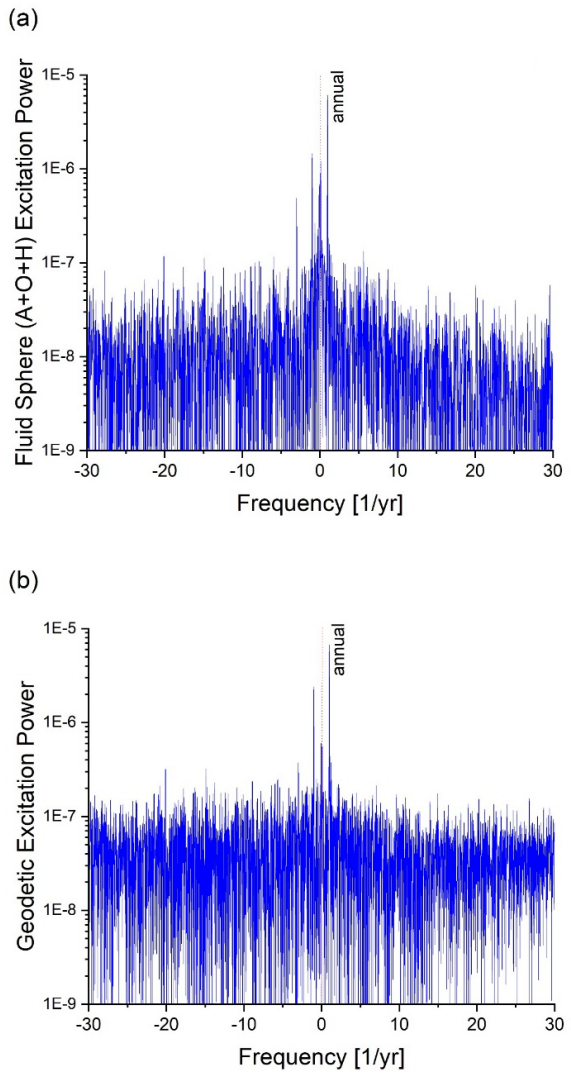

Fig. A2. Two power spectra of excitation functions: (a) Fluid spheres excitation, (b) Geodetic excitation.

APPENDIX 3

Seismic Excitation of Polar Motion

The seismic moment tensor M_{ij} for an earthquake of principal seismic moment M_k, is given as

$$M_{ij} = \sum_{k=1}^{3} A_{ik}\, A_{jk}\, M_k \tag{A15}$$

where the coordinate transform matrix A_{ij} is defined as

$$\begin{bmatrix} -sin(pl_1) & -sin(pl_2) & -sin(pl_3) \\ -cos(pl_1)\cos(az_1) & -cos(pl_2)\cos(az_2) & -cos(pl_3)\cos(az_3) \\ cos(pl_1)\sin(az_1) & cos(pl_2)\sin(az_2) & cos(pl_3)\sin(az_3) \end{bmatrix} \tag{A16}$$

with az_i and pl_i as the azimuth and plunge of i-th principal direction. M_{ij} is the seismic moment tensor in the spherical coordinate frame $(\hat{r}, \hat{\theta}, \hat{\varphi})$. In the USGS earthquake catalog, the azimuth and plunge angles are given in $(\hat{n}, \hat{e}, \hat{z})$ frame. Two frames are related as $(\hat{r}, \hat{\theta}, \hat{\varphi}) = (-\hat{z}, -\hat{n}, \hat{e})$.

The perturbations in the two off-diagonal inertia tensor components of the Earth due to an earthquake were expressed after Gross (1986) as

$$\begin{aligned} \Delta I_{13} = {} & \Gamma_1 \left[\frac{1}{2}\left(M_{\theta\theta} - M_{\varphi\varphi} \right) \sin 2\theta \, \cos\varphi - 2M_{\theta\varphi} \sin\theta \, \sin\varphi \right] \\ & - \Gamma_2 M_{rr} \sin 2\theta \, \cos\varphi \\ & + \Gamma_3 \left[-M_{r\theta} \cos 2\theta \, \cos\varphi + M_{r\varphi} \cos\theta \, \sin\varphi \right] \end{aligned} \tag{A17}$$

$$\begin{aligned} \Delta I_{23} = {} & \Gamma_1 \left[\frac{1}{2}\left(M_{\theta\theta} - M_{\varphi\varphi} \right) \sin 2\theta \, \sin\varphi + 2M_{\theta\varphi} \sin\theta \, \cos\varphi \right] \\ & + \Gamma_2 M_{rr} \, \sin 2\theta \, \sin\varphi \\ & - \Gamma_3 \left[M_{r\theta} \cos 2\theta \, \sin\varphi + M_{r\varphi} \cos\theta \, \cos\varphi \right] \end{aligned}$$

where $M_{\mu\nu}$ are the same as above and Γ_i are focal depth dependent parameter determined by the physical properties of the Earth's interior. Given the perturbation ΔI_{i3} due to earthquakes, the corresponding coseismic excitation is readily found according to the Eq. (2).

The post seismic deformation and corresponding polar motion excitation can be approximated by simple homogeneous relaxation model (Na & Kyung 2016).

$$u(t) = u_0 + u_1\left(1 - e^{-t/\tau}\right) \tag{A18}$$

The constants here were adopted as $u_1 = 0.655u_0$ for τ = 125 days, while their lower and upper bound can be taken as

$u_1 = 0.524u_0$ for $\tau = 80$ days and $u_1 = 0.820u_0$ for $\tau = 200$ days after Hearn (2003) and the observed crust relaxation after 2010 Tohoku Earthquake (Na & Kyung 2016).

The calculated coseismic excitation by the 37 largest earthquakes since 1980 until Spring 2025 are listed in the Table A1. The information of epicenter, magnitude, and focal depth for each earthquake, which were acquired from the USGS data center, are listed together in the table. The two components χ_1 and χ_2 - the coseismic polar motion excitations have been calculated by using Eq. (2) with the formulae shown above.

Table A1. The largest earthquakes (M > 8) since 1980 until Spring 2025 and their coseismic polar motion excitation. Each occurrence date and location, magnitude, focal depth [km], and the calculated coseismic excitation (χ_1, χ_2). Unit of excitation: [milliarcsec]

Date	Region	Lat, Lon	Mag, Dep	χ_1 and χ_2	
1985.3.3	Chile	33.14S, 71.87W	7.9, 40.7	–0.044	0.124
1985.9.19	Mexico	18.19N, 102.53W	8.0, 21.3	0.005	–0.065
1986.5.7	Aleutian	51.52N, 174.78W	7.9, 31.3	–0.094	0.009
1989.5.23	Australia	52.34S, 160.57E	8.2, 15.0	0.061	–0.047
1994.6.9	Bolivia	13.84S, 67.55W	8.2, 651.	–0.043	0.068
1994.10.4	Kuril	43.77N, 147.32E	8.3, 60.5	–0.188	0.215
1995.7.30	Chile	23.34S, 70.29W	8.0, 30.5	–0.046	0.112
1995.10.9	Mexico	19.06N, 104.21W	7.9, 13.5	0.006	–0.042
1996.2.17	Indonesia	0.89S, 136.95E	8.1, 11.5	–0.014	–0.032
1998.3.25	Australia	62.88S, 149.52W	8.1, 17.5	–0.049	–0.117
2000.11.16	Papua NG	3.98S, 152.17E	8.0, 23.5	0.020	0.032
2001.6.23	Peru	12.27S, 73.64W	8.4, 23.5	0.063	0.234
2003.9.25	Japan	41.82N, 143.91E	8.2, 23.5	–0.083	0.129
2004.12.23	Australia	49.31S, 161.35E	8.1, 13.5	0.091	0.055
2004.12.26*	Sumatra	2.30N, 95.98E	9.1, 13.5	–0.623	0.561
2005.3.28*	Sumatra	2.09N, 97.11E	8.6, 30.5	–0.180	0.082
2006.5.3	Tonga	20.19S, 174.12W	8.0, 60.5	0.069	0.031
2006.11.15	Kuril	46.59N, 153.27E	8.3, 11.5	–0.227	0.186
2007.1.13	Kuril	46.24N, 154.52E	8.1, 11.5	0.120	–0.113
2007.4.1	Solomon	8.47S, 157.04E	8.1, 21.5	0.030	–0.992
2007.8.15	Peru	13.39S, 76.60W	8.2, 25.5	0.015	0.778
2007.9.12	Sumatra	4.44S, 101.37E	8.4, 30.5	–0.099	–0.026
2009.9.29	Sumatra	15.49S, 172.10W	8.1, 15.5	–0.106	0.042
2010.2.27*	Chile	36.12S, 72.90W	8.8, 30.5	–0.776	2.028
2011.3.11*	Japan	38.30N, 142.38E	9.1, 11.5	–2.064	2.356
2012.4.11*	Sumatra	2.33N, 93.06E	8.6, 30.5	0.707	0.046
2012.4.11	Sumatra	0.80N, 92.46E	8.2, 53.7	0.196	–0.006
2013.2.6	Solomon	10.80S, 165.11E	8.0, 15.0	0.027	–0.036
2013.5.24	Okhotsk	54.90N, 153.22E	8.3, 610.	–0.002	–0.317
2014.4.1	Chile	1.61S, 70.77W	8.2, 25.5	–0.021	0.092
2015.9.16	Chile	31.57S, 71.67W	8.3, 22.4	–0.102	0.299
2017.9.8	Mexico	15.02N, 93.90W	8.2, 45.5	–0.054	0.096
2018.8.19	Fiji	18.11S, 178.15W	8.2, 580.5	–0.098	–0.052
2019.5.26	Peru	5.81S, 75.27W	8.0, 130.5	–0.020	–0.046
2021.3.4	Kermadec	29.72S, 177.28W	8.1, 23.5	0.157	0.022
2021.7.29	Alaska	55.36N, 157.89W	8.2, 35.5	–0.157	–0.022
2021.8.12	Sandwich I.	58.38S, 25.25W	8.1, 10.0	–0.074	0.012

* greatest earthquakes (M > 8.5).

APPENDIX 4

JPL Long Polar Motion Data and Geomagnetic Jerks

To analyze the phase variation of Chandler wobble, we used a long-time dataset JPL pole 2021. By using a frequency window, we extracted Chandler wobble from the given polar motion time series. Two components of the extracted Chandler wobble are shown below (Fig. A3).

We designed two wavelets of sine and cosine functions of Chandler period confined in a longer cosine bell envelope as shown in the next figure (Fig. A4). In fact, we tested a narrower wavelet as well, but the calculation result was almost the same. Convolving the wavelets with the pole 2021

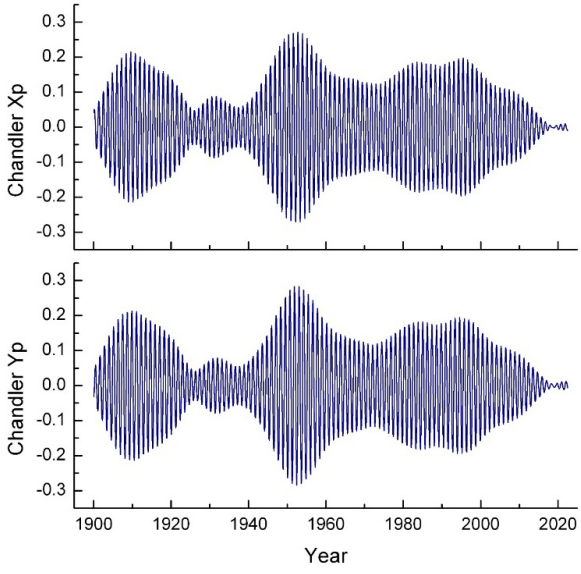

Fig. A3. Chandler wobble extracted from the JPL pole 2021 time series by filtering (unit: arcsec).

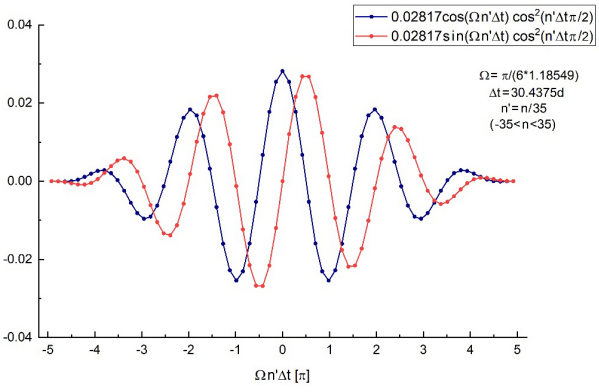

Fig. A4. Wavelet used for assessment of amplitude and phase of Chandler wobble.

dataset, we identified the long-term variation of amplitude and phase of Chandler wobble. The acquired amplitude and phase variations are shown below, where the epochs of known geomagnetic jerks (Gibert & Le Mouël 2008; An & Ding 2022) are marked with dotted lines (Fig. A5).

The phase of Chandler wobble changed fast at two periods: (i) between 1922 and 1940 and (ii) after 2015. And the abrupt phase change after 2015 is, as a matter of fact, associated with the amplitude decrease during the same time. Other fast phase variations near 1927 and 1938 are also associated with the amplitude decrease. However, except these large changes, the Chandler phase has been moderate and slowly changing for more than 60 yr between 1945 and 2015, and it did not have any evident correlation with the geomagnetic jerks during those years.

After a numerical simulation of geomagnetic jerk, the typical amount of torque associated with geomagnetic jerk has been found as about 1×10^{16} [Nm] (Aubert & Finlay 2019). With one year duration, which is also a typical time span of the simulated jerk, the torque would result in a pole shift of 5.4×10^{-11} rad = 0.011 milli arcsec, which corresponds to 0.34 mm at the surface of the Earth. These are the maximum possible values when the jerk affects in the most effective direction. Yet the amount is even smaller by one or two order of magnitude than the largest seismic excitation (see Table A1). Moreover, geomagnetic jerk occurs along a time span of one year or so, while coseismic displacement occurs within minutes time. Therefore, geomagnetic jerk cannot be regarded as phase changer or noticeable energy source of Chandler wobble.

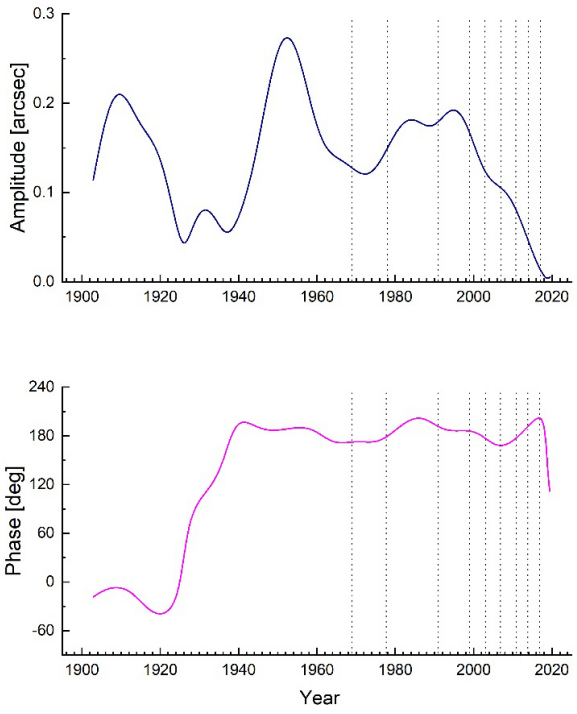

Fig. A5. Amplitude and phase variation of Chandler wobble shown together with the known geomagnetic jerks.